Comparative studies of ethylene–α-olefin copolymers by thermal fractionations and temperature-dependent crystallinity measurements

P. Starck[*], K. Rajanen, B. Löfgren

Helsinki University of Technology, Polymer Science Centre, Innopoli B2, P.O. Box 356, 02151 Espoo, Finland

Abstract

In this work the crystallization behavior and thermal fractionation results of various ethylene–α-olefin copolymers (1-butene, 1-hexene, 1-octene, 1-tetradecene, 1-hexadecene, 1-octadecene, vinylcyclohexane as comonomer) were evaluated using differential scanning calorimetry (DSC). The step crystallization (SC) method was compared with the successive self-nucleation/annealing (SSA) method. SSA exhibited better separation than SC, especially in the low temperature regions, and provided results in a shorter time. The temperature-dependent crystallinities confirmed that for all more branched polymers a lot of material is present at ambient and can crystallize below that temperature. Significant differences in the temperature-dependent crystallinity curves existed between ZN- and metallocene-catalyzed copolymers at the same comonomer level (and comonomer type).
© 2002 Elsevier Science B.V. All rights reserved.

Keywords: Step crystallization; Successive self-nucleation/annealing; DSC; Ethylene–α-copolymer; Temperature-dependent crystallinity

1. Introduction

Multiple melting peaks are frequently observed in the differential scanning calorimetry (DSC) endotherms of crystalline and semicrystalline polymers. Already in 1964, Gray and Casey [1] reported on the influence of thermal history on the melting curves of polyethylene. These early findings have during the last 10–12 years lead to the use of DSC fractionation techniques as a possible alternative to temperature rising elution fractionation (TREF) [2] and/or crystallization analysis fractionation (CRYSTAF) [3]. Studies on the chain branch distribution and the sequence length between the chain branches in ethylene–α-copolymers have been done using methods based on a special heat treatment (annealing) of the samples and the subsequent analysis of melting behavior by DSC. In these methods a particular thermal treatment on the samples, such as stepwise isothermal segregation technique (SIST) [4], stepwise cooling (also called stepwise crystallization or SC) [5–13], or successive self-nucleation/annealing (SSA) [14–18], were applied. Typical for all these fractionation methods is that the crystallization at each isothermal step depends on the segment length between branches [7,19]. As the comonomer content increases, the resulting shorter sequences cause the copolymer molecules to crystallize at lower and lower temperatures and in smaller and smaller, less and less perfect structures. Corresponding ethylene length sequence distributions give rise to a multi-SC resulting in

---

[*] Corresponding author.

several crystal (lamellae) thickness populations, which are reflected as a multiple peaked melting point distribution. Therefore, we see a separation according to the branching densities in a subsequent heating scan. These thermal fractionation methods can provide a more exact, although qualitative; information on the short chain branching (SCB) distribution of the polymer, than conventional DSC. Recent studies by Gabriel and Lilge [20] and Lustiger et al. [21] have further emphasized the good correlations between DSC fractionation methods, and TREF and CRYS-TAF, in determinations of the comonomer distributions in polyethylenes.

Müller et al. [14], in their primary work on SSA, claimed that SSA provides better fractionation than the SC of ethylene–1-butene and ethylene–1-octene copolymers. As our earlier SC studies have been extended to ethylene copolymers of a wide range of comonomer types from 1-butene to 1-octadecene [8,10,22–24], moreover to functional comonomers [25], covering both low and high comonomer contents, the current work tries to implement the SSA method in order to further support the studies of our copolymers.

The short chain branches (SCBs) in homogeneous ethylene copolymers have a predominant effect on crystallization and melting. This is not reflected only in the crystallization and melting, but also in the temperature-dependent degree of crystallinity. Crystallinity will increase with temperature during cooling from the melt and decrease with temperature during immediate reheating of samples crystallized by cooling at constant rate. It has been emphasized [26–29] that ethylene–α-copolymers may exhibit crystallization and melting in the sub-ambient region and that incorrect, too low crystallinity values are obtained when fixed values at the equilibrium melting point, T_m^0, are calculated with the peak area method by DSC. Therefore, the temperature-dependence of enthalpies has been determined [26,27] in order to give more accurate calculations of crystallinities. The methods to determine the temperature-dependent crystallinities have been largely discussed and further developed by Mathot et al. [27–32]. In this work, we use an "extrapolation method" [32] for the calculations of crystallinities in order to get further information on the crystallization behavior of our different ethylene copolymers.

2. Experimental

2.1. Materials

The polymers studied consisted of commercial Ziegler–Natta (ZN) catalyzed linear low density polyethylene (LLDPE) and very low density polyethylene (VLDPE) samples as well as both commercial metallocene (Me)-catalyzed and experimentally synthesized Me-catalyzed polyethylenes. Two commercial Me ethylene–1-octene copolymers, EO5 and EO6, were produced using constrained geometry catalyst technology (CGCT) catalysts [33]. Our synthesized Me copolymers were produced in lab-scale polymerizations. The lab-scale polymerizations are described in previous studies [34–37]. All polymers studied are listed in Table 1.

3. Characterization

3.1. Conventional DSC

All melting and crystallization studies were made with a Perkin-Elmer DSC-7 differential scanning calorimeter (DSC). The temperature calibration was made with indium (m.p. 156.6 °C) and for the temperature/area calibration the heat capacity value 28.45 J/g was used. Crystallinity values were determined from the integral area of the melting range and the value 293 J/g [38] was used as the enthalpy of fusion of perfectly crystalline polyethylene. The DSC runs of the samples were carried out under the following conditions: (1) fast heating to 160 °C, (2) hold for 2 min, (3) cooling from 160 to 10 °C at 10 °C/min, (4) hold for 1 min, (5) heating at 10 °C/min from 10 to 160 °C. The melting points and crystallinity values X_c (a) in Table 1 are from the second heating scans.

3.2. Step crystallizations

The SCs, carried out using DSC, were performed according to procedures described earlier [8,10]. In this method, the sample was annealed (120 min at each temperature) in steps at successively lower annealing temperatures (temperature stages separated from each other by 6 °C). As the melting ranges of the studied polymers varied a lot due to different

Table 1

Basic characteristics of studied copolymers. X_c (a) represents crystallinities obtained with the conventional peak area method and X_c (b) represents crystallinities at 25 °C, obtained with the extrapolation method[a]

Sample	Catalyst/ process	Comonomer		Density (kg/m³)	M_w (kg/mol)	Melting point (°C)	X_c (a) (%)	X_c (b) (%)	Reference
		Type	mol%						
EB1-ZN	ZN/Com	1-Butene	4.2	920	116	124	41	48	[8]
EB2	Me/Com	1-Butene	5.5	905	76	96	35	39	[8]
EB3	Me/Com	1-Butene	7.4	899	96	85	27	31	[43]
EB4	Me/Com	1-Butene	8.2	895	74	87	28	32	[8]
EB5-V	V/Com	1-Butene	9.2	888	68	70	19	24	[8]
EB6	Me/Com	1-Butene	12.6	881	80	47	14	16	[43]
EH1	Me/Lab	1-Hexene	0.6	939	102	125	58	66	[35]
EH2	Me/Lab	1-Hexene	1.9	927	112	115	46	53	[35]
EH3	Me/Lab	1-Hexene	4.3	904	86	100	31	n.a.	[36]
EH4	Me/Lab	1-Hexene	5.3	903	88	97	30	37	[36]
EH5	Me/Lab	1-Hexene	12.5	874	71	60	11	12	[36]
EH6	Me/Lab	1-Hexene	17.3	856	128	n.d.	n.d.	3	[36]
EO1	Me/Lab	1-Octene	1.9	934	81	116	48	55	[34]
EO2-ZN	ZN/Com	1-Octene	2.6	920	125	125	43	46	[8]
EO3	Me/Lab	1-Octene	3.5	923	79	106	40	46	[34]
EO4-ZN	ZN/Com	1-Octene	3.8	912	89	125	35	37	[43]
EO5	Me/Com	1-Octene	6.2	898	75	95	30	36	[43]
EO6	Me/Com	1-Octene	11.8	884	48	77	18	21	[43]
ETD1	Me/Lab	1-Tetradecene	2.3	923	74	116	47	54	[34]
ETD2	Me/Lab	1-Tetradecene	5.0	900	72	94	23	26	[34]
EHD1	Me/Lab	1-Hexadecene	1.1	922	74	120	48	52	[36]
EHD2	Me/Lab	1-Hexadecene	3.4	906	64	101	37	42	[36]
EHD3	Me/Lab	1-Hexadecene	5.9	896	77	91	26	30	[36]
EOD1	Me/Lab	1-Octadecene	2.0	927	67	113	41	49	[34]
EOD2	Me/Lab	1-Octadecene	4.8	903	65	91	34	37	[37]
EVCH1	Me/Lab	Vinylcyclohexane	1.4	926	124	120	49	52	[37]
EVCH2	Me/Lab	Vinylcyclohexane	3.4	917	116	111	39	43	[37]
EVCH3	Me/Lab	Vinylcyclohexane	6.5	916	217	107	11	n.a.	[37]

[a] Lab: laboratory polymerization; Com: commercial product; n.a.: not analyzed; n.d.: not detected.

comonomer contents, the crystallization (annealing) temperatures, T_c, were chosen to observe the highest number and best resolved melting endotherms in the melting curves of each sample. The isothermal crystallization ranges used in the present study were from 128 to 80, 104 to 56, 98 to 50 or 86 to 38 °C, followed by cooling to ambient. After the annealing steps, the melting curve of the polymer was obtained by heating the cooled sample at a heating rate of 10 °C/min up to 150 °C, and the melting peaks, with the corresponding heights of the separated peaks, were analyzed. Because the crystallization (annealing) steps in the SC-method, on average, lasted about 18 h the fractionation was done over night. Longer annealing times (>120 min) and a slower heating rate (5 °C/min) give a

slightly better separation of peaks [8] but is more time consuming.

3.3. Successive self-nucleation/annealing measurements

The SSA procedure using DSC followed the principles of Müller and coworkers [14,15]. The samples with "identical" thermal history were first cooled down from 160 to 30 °C at 10 °C/min, hold there for 1 min. Subsequently, a heating at a scan rate of 10 °C/min was performed up to a selected self-seeding and annealing temperature denoted as T_s, where the sample was isothermally kept for 5 min before cooling it again at 10 °C/min down to 30 °C (to 10 °C in the

analyses of some highly branched samples). At the end of the first cooling from T_s, the polymer has been self-nucleated [14,39]. Then the sample was heated in the DSC again at 10 °C/min, but this time up to new T_s, which was 6 °C lower than the previous T_s. This means that the unmelted crystals at this lower T_s will anneal during the 5 min at this temperature, some of the melted species will isothermally crystallize (after being self-nucleated by the unmelted crystals), while the rest of the molten crystallizable chains (or chain segments) will only crystallize during the subsequent cooling from T_s. This procedure is then repeated with T_s again being lowered at 6 °C intervals (same stages as in the SC fractionations!) with respect to the previous step. The chosen T_s range was from 128 to 62, 122 to 44, 110 to 44, and 86 to 14 °C. Finally, the melting behavior was recorded when the thermal conditioning was over. A typical fractionation by SSA lasted about 4 h; this made two SSA fractionations possible during a normal working day.

The most important parameters in using the SSA method are the first T_s temperature to be used, the temperature interval between T_s temperatures, the permanence time at T_s and the heating rates during the thermal conditioning steps [17]. A spacing of 3 °C instead of 6 °C had probably given a slightly better separation and more peaks, but we wanted to keep the annealing steps similar to those of the SC procedure. An increase in holding time does not promote higher number of signals, but more perfect crystals are expected at higher time consumption.

3.4. Temperature-dependent crystallinity

For the calculation of the crystallinity as a function of temperature, in both cooling and heating, we used an extrapolation method as applied to pseudo-heat capacity measurements [32]. In this method, extrapolation from the melt is used to estimate the contribution to the signal of the (100%) amorphous phase. No heat capacity measurements are requested using the commercially available software package [40], which uses a two-phase model (where molecules are expected to be either in an amorphous or crystalline phase). Effective corrections for "instrumental curvature" are requested for quantitative measurements [32,40,41], and therefore an empty-pan measurement was subtracted from all sample

measurements in order to obtain a first order correction for instrumental curvature of the DSC curves applied.

Moreover, emphasis was put on negligible ambient influences by taking care of cooling unit and temperature fluctuations in laboratory. Due to these circumstances, we did not extend our experiments to start below −20 °C, although results by Mathot and Pijpers [28] have demonstrated that differences in crystallinity of VLDPEs can be seen already above −60 °C. The crystallinities from the temperature-dependent melting curves, taken at ambient ($T = 25$ °C), are given as X_c (b) in Table 1.

4. Results and discussion

4.1. Comparison of SC and SSA fractionations

The results from a comparative study of the two fractionation methods, as applied on two ZN ethylene–1-butene copolymers, are exhibited in Fig. 1. Both methods display a separation of peaks due to segregation by ethylene sequence length, but the SSA methods gives more separated and sharper peaks. The high temperature peaks of the heterogeneous EB1-ZN correspond to unbranched or weakly branched molecules, the low temperature endotherms being associated to branched molecular species. SSA of EB1-ZN exhibits nine separated peaks between 128 and 78 °C, but SC only six peaks between 128 and 93 °C. The use of SSA seems to be a more efficient method, especially in the separation of more branched species, which have smaller and less perfect structures. This efficiency is noticed from the SSA curve of the sample EB5-V, which exhibits 10 peaks from 90 to 37 °C, as SC gives only six resolved peaks from 77 to 47 °C. The comonomer distribution of this vanadium catalyzed VLDPE is homogeneous in accordance with earlier results [5,8,22,34].

Fig. 2, comparing the two methods on Me-catalyzed ethylene–1-butene copolymers, shows the efficiency of the SSA method, which is more pronounced for copolymers of higher comonomer content. SSA of the VLDPE EB6 shows seven separated, although weak peaks, which according to recent studies [32,42,43] most probably do not correspond to lamellar structures, but to bundled crystals. Minick et al. [42] have
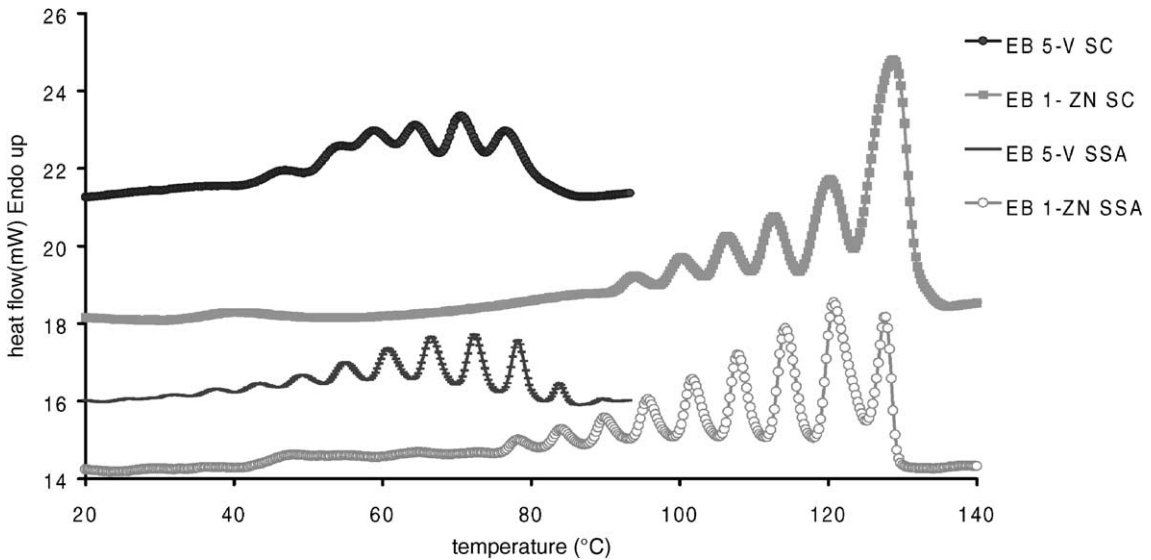
Fig. 1. DSC endotherms of two ZN-catalyzed ethylene–1-butene copolymers, obtained after SCs and SSA, respectively.

demonstrated that even in CGCT copolymers of very low density, these bundled crystals recrystallize during isothermal annealing. The efficient separation of EB6 in the low temperature region by SSA supports such as recrystallization.

Fig. 3a and b demonstrates that the efficiency of the two fractionation methods is about the same for a Me ethylene–1-hexene copolymer with low comonomer content (EH2) (five separated peaks), but for samples containing more 1-hexene, the SSA method is again more useful (EH3: seven separated peaks (SSA) vs. five separated peaks (SC)). An increase in comonomer content from 4.3 (EH3) to 5.3% (EH4) gives an additional peak and a change in the ethylene sequence
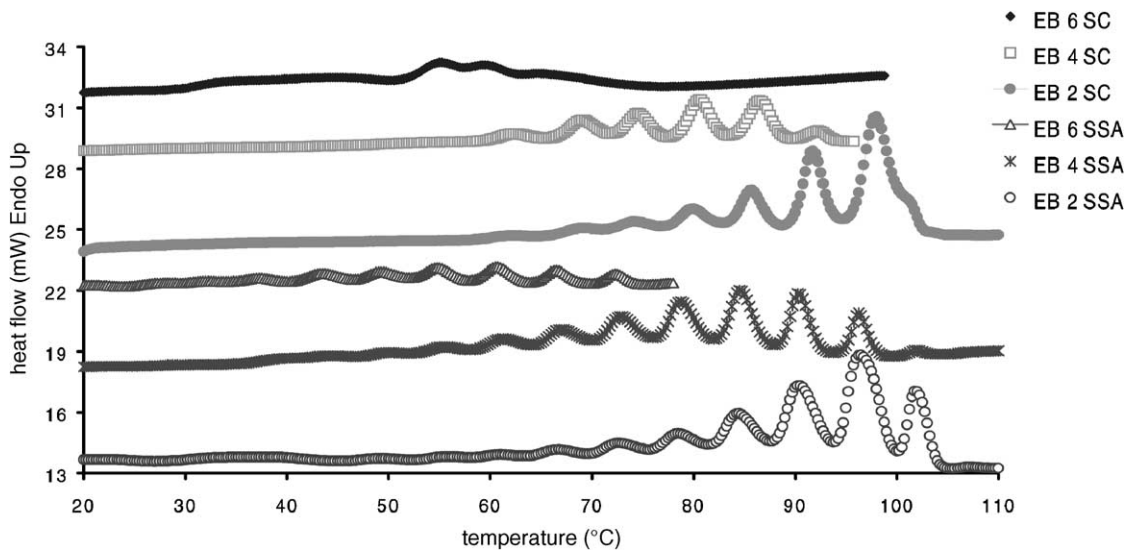
Fig. 2. DSC endotherms of Me-catalyzed ethylene–1-butene copolymers, obtained after SC and SSA, respectively.
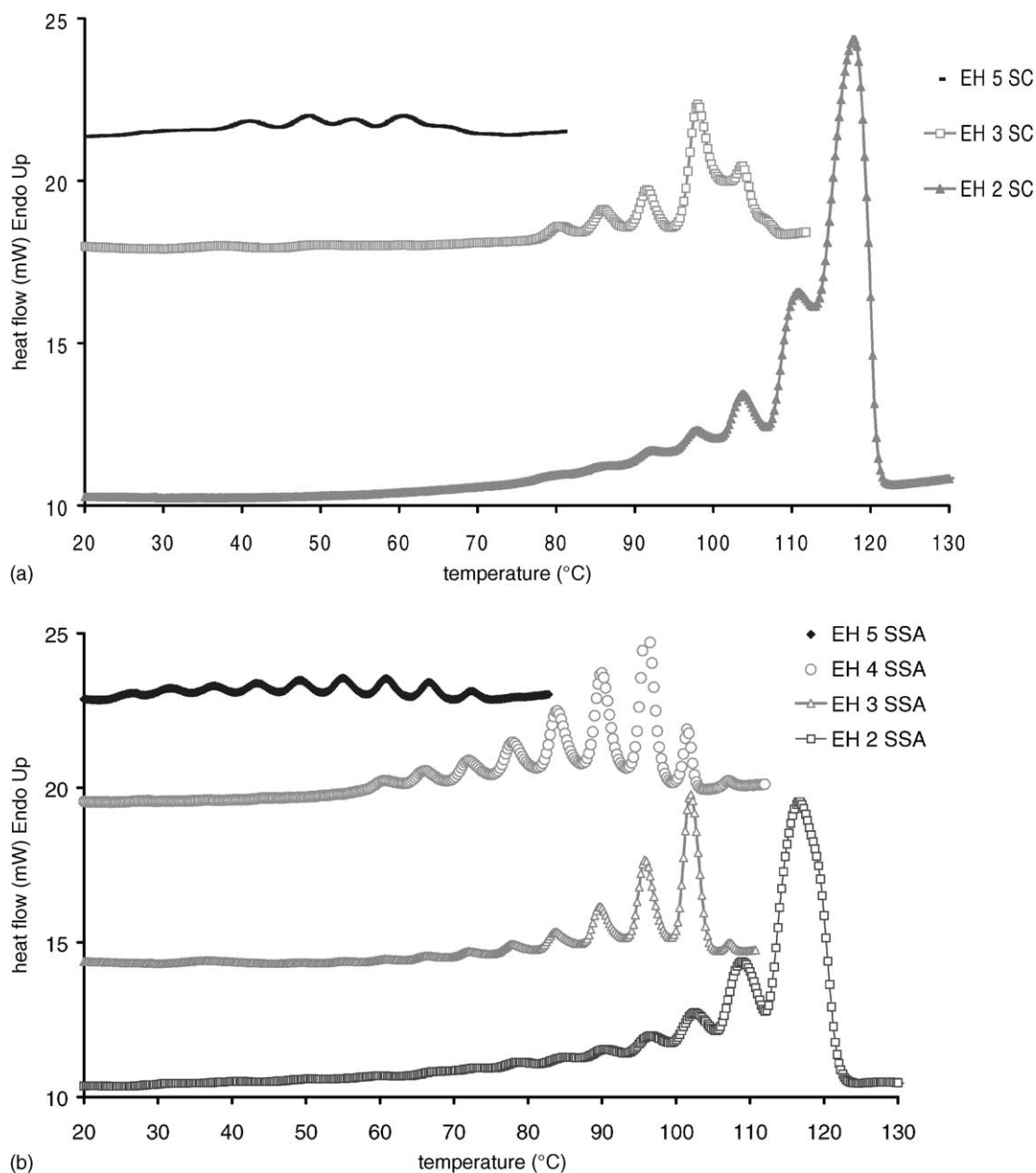
Fig. 3. DSC endotherms of ZN- and Me-catalyzed ethylene–1-octene copolymers, obtained after fractionations: (a) SC; (b) SSA.

length causes a shift in the ranges of the peak temperatures from 107–66 to 102–61 °C. No melting peak was detected in the endotherm of the virgin, unfractionated sample EH5, but SSA of this sample exhibits seven separated, although weak peaks. The better separation of the SSA method as compared to SC is suggested by Müller et al. [14] to be due to the partial melting steps that are performed after the dynamic crystallization, which follows each period at the self-seeding/annealing temperature T_s.

Comparisons of ethylene–1-octene copolymers, studied by SSA and SC, are given in Fig. 4a and b.
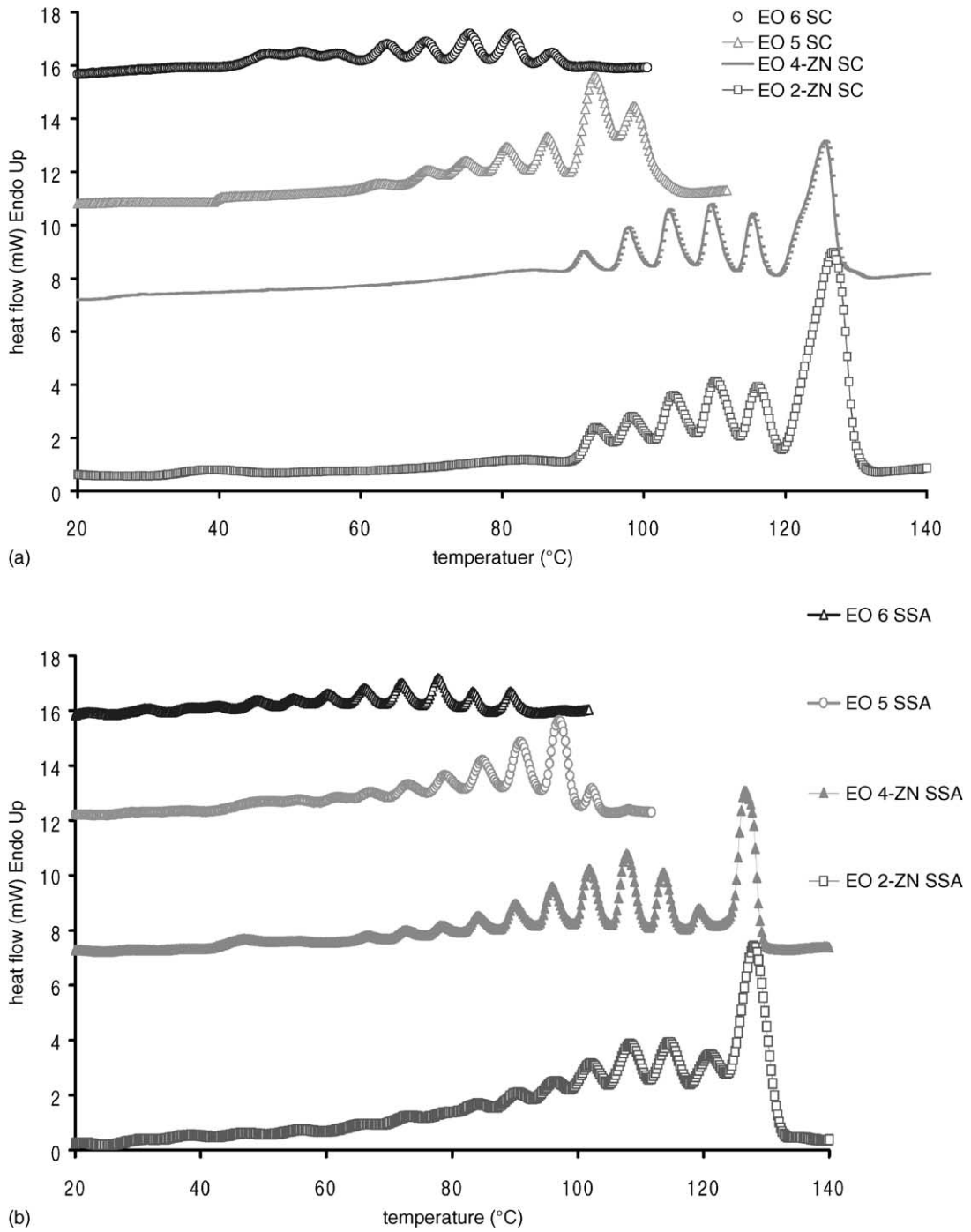
Fig. 4. DSC endotherms of Me-catalyzed ethylene–1-hexene copolymers, obtained after fractionations: (a) SC; (b) SSA.
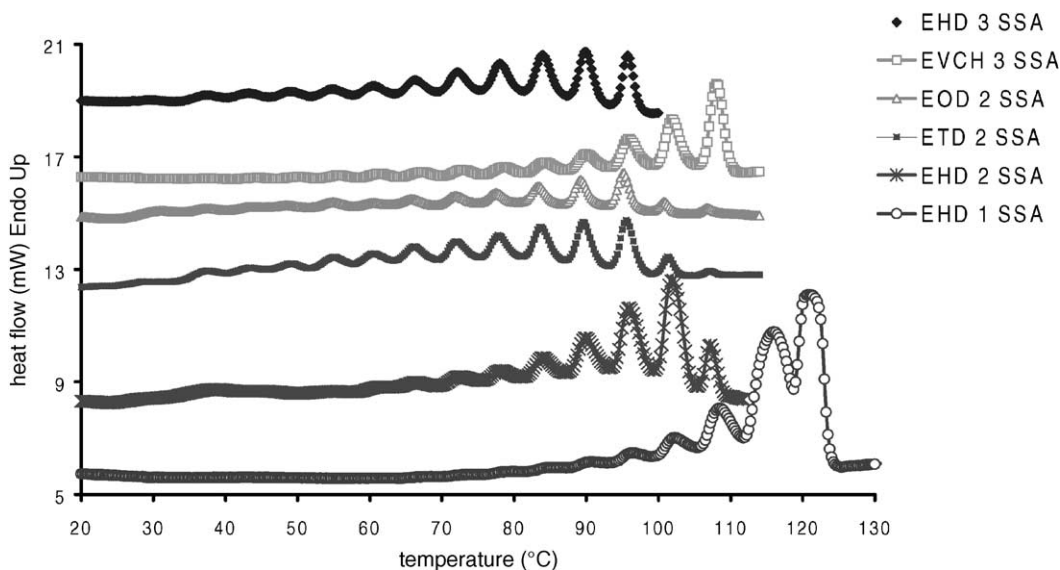
Fig. 5. DSC endotherms of Me-catalyzed ethylene/long chain copolymers, obtained after SSA fractionations.

The presence of the linear molecular species is clearly seen in both curves of the two ZN copolymers, EO2-ZN and EO4-ZN, but the CGCT catalyzed Me copolymers, EO5 and EO6, exhibit homogeneous comonomer distributions by both methods. SSA of the slightly branched ZN-catalyzed copolymers, characterized by broad sequence length distributions [44], show 10 separated peaks for EO2-ZN and 11 peaks for EO4-ZN. This is somewhat more than what is exhibited for Me copolymers of about similar comonomer content (for instance EH2 and EH3 in Fig. 3b), but is caused by their much shorter ethylene sequences.

The endotherms after SSA fractionations, of ethylene/long chain α-olefin—and ethylene/vinylcyclohexane copolymers, are presented in Fig. 5. SC fractionations of EOD2 and ETD2 gave according to a recent paper [24], where these polymers were named OD6 and TET10, eight (EOD2) and six (ETD2) separated peaks, and the results of SSA applied, gave nine and 10 peaks, respectively. SSA displays also a slightly better separation of EVCH3 compared to SC (seven resolved peaks by SSA and five peaks by SC). Our recent results [37] have demonstrated that SSA, applied on ethylene/vinylcyclohexane copolymers, is able to reveal differences in the comonomer distributions of this type of copolymers.

Most of our comparisons support the findings of Müller et al. [14] concerning the efficiency of SSA compared with SC, but the differences are not very significant for all types of copolymers. The fact that they presented a much bigger difference in the efficiency of the two fractionation methods may be partly due to their short crystallization times, 5 min, used at each crystallization temperature, T_c. In our work, we used a much longer time, 120 min, and even crystallization (annealing) times up to 12 h have been reported [7], in order to confirm a complete annealing.

4.2. Temperature-dependent crystallinities

The introduction of higher amounts of branches (defects) in the polymer chains will cause a reduced length of sequences able to crystallize. Our data in Table 1 clearly demonstrate that this will lead to a decrease in melting temperature and level of crystallinity, and this is true for all the comonomers included in our study.

The extrapolation method used for the determinations of temperature-dependent crystallizations is expected to provide more information of existing material in the sub-ambient region. This method enables an analyst independent determination of the crystallinity as a function of temperature in both

cooling and heating. The enthalpy of transition decreases with decreasing temperature, by which the crystallinity will be increased with decreasing temperature. However, on the other hand, a crossing of the extrapolation line with the DSC curve will lead to a decrease in the total area of the melting endotherm, and the crystallinity will be decreased [40]. In spite of this canceling of errors, somewhat higher crystallinities could result by using the extrapolation method.

Fig. 6a clearly demonstrates that the maximal crystallinities at low temperatures can be considerably
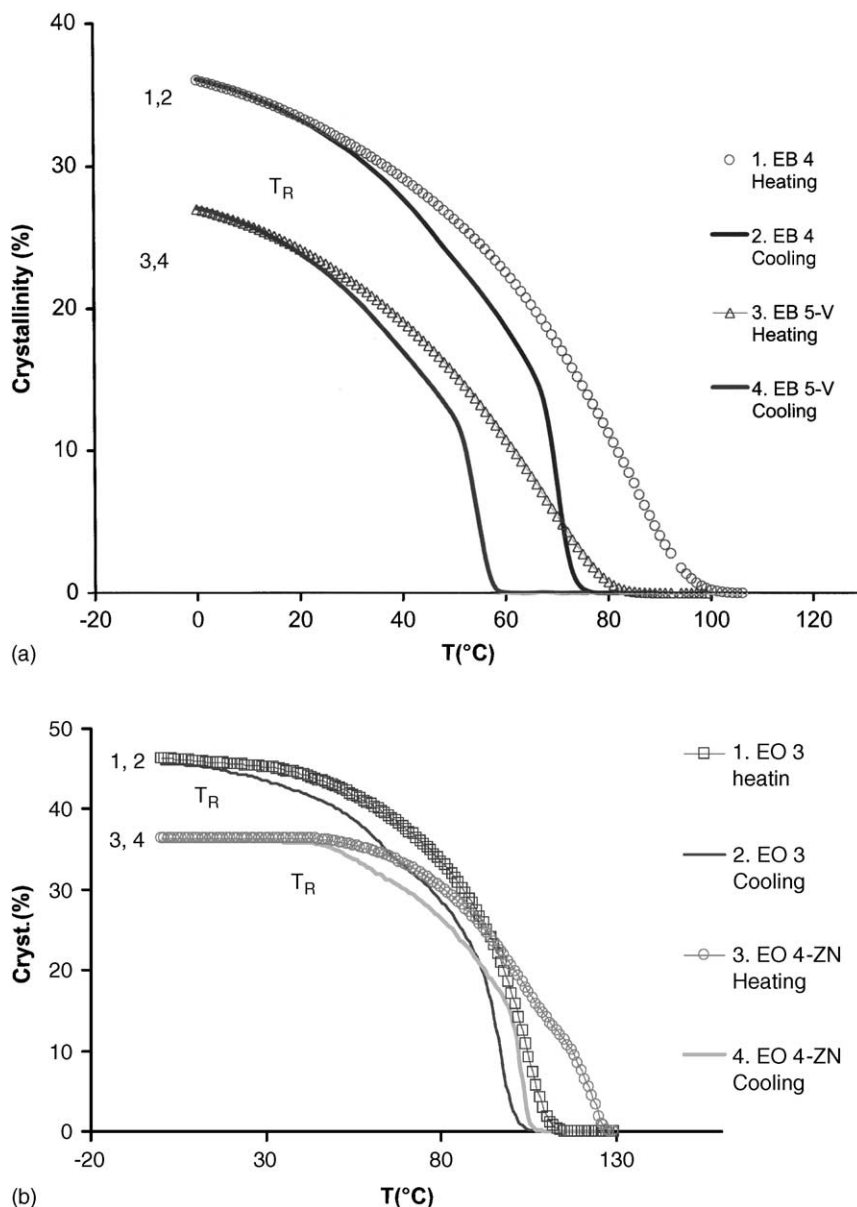

Fig. 6. Temperature-dependent crystallinities of ZN and Me copolymers on cooling and heating: (a) ethylene–1-butene copolymers; (b) ethylene–1-octene copolymers.

higher than at room temperature, which means that there is still a lot of material present at ambient, which can crystallize below that temperature. For the samples in Fig. 6a the butene segments hinder crystallization at higher temperatures and the same behavior exists to an even higher extent for copolymers synthesized with longer comonomers. The maximal crystallinities after cooling and heating are the same as is shown from the cycles in the figure. The largest change in crystallinity occurs at high temperature in the hysteresis loop, but the crystallinity profiles of the two polymers have the same shapes, which is not unexpected because the vanadium catalyzed sample EB5-V also has a homogeneous comonomer distribution, as is the case for the Me-catalyzed polymer EB4. The smaller crystallinity values X_c (a) and X_c (b) (Table 1) of EB5-V are in accordance with the slightly lower density values, lower comonomer content, and position of the crystallinity profiles, compared to EB4. Mathot et al. [31,41] concluded from studies on two homogeneous ethylene–1-octene copolymers, polymerized with vanadium and Me catalyst, respectively, that identical crystallinity curves as function of temperature indicate very similar ethylene sequence distributions. A comparison of the SSA curves of EB5-V (Fig. 1) and EB4 (Fig. 2) demonstrate the similarity in the shapes of the curves, but EB4 displays some higher melting populations at 90 and 96 °C, which are in accordance with the crystallinity results.

Alizadeh et al. [45] found in their studies on ethylene–1-octene copolymers that the change in crystallinity during cooling becomes more significant in the low temperature and less in the high temperature hysteresis region when the octene content is raised. They also found that the onset temperature for the reversible crystallinity change decreases with increasing octene content and is identical with a crossover temperature, T_R, where the crystallinity becomes independent of cooling rate. T_R is the temperature where the transition in the crystallization mechanism is observed (see Fig. 6a and b). Despite the differences in X_c (a) and X_c (b) values, our copolymers EB4 and EB5-V in Fig. 6a display very similar T_R temperatures. This is not unexpected as they contain very similar comonomer amounts.

Fig. 6b compares the crystallinity curves of a ZN-catalyzed ethylene–1-octene copolymer EO4-ZN with a Me-catalyzed copolymer EO3 with about the same comonomer content. We notice an increase in crystallinity as a result of crystallization in cooling and a decrease as a result of melting in heating, but EO4-ZN, with a significant linear tail in the SC and SSA curves (as well as in its DSC endotherm), shows a very insignificant increase in crystallinity below ambient. The crystallinity values between cooling and heating above about 90 °C differ much more for the ZN-catalyzed copolymer, which may be due to the relatively high amount of linear species existing in this polymer. The T_R temperature for the ZN copolymer is significantly higher than corresponding temperature for EO3, which also demonstrates the slower crystallization rates of Me polymers.

The temperature-dependent crystallinity curves of six ethylene–1-butene copolymers in Fig. 7 and their data in Table 1 demonstrate a relationship for dependence of melting point and crystallinity at different temperatures. McKenna [46], in his studies on crystallinity data as a function of temperature, found a strong relationship for dependence of melting point and residual crystallinity at 20 °C for ethylene–1-butene copolymers. Our results in Table 1 confirm, with exception of EB6, clear differences existing in crystallinities obtained from peak area calculations, X_c (a), and temperature-dependent measurements, which are in accordance with information given by Peeters et al. [30]. The differences between X_c (a) and X_c (b) are in the range 2–9%. At sub-ambient temperatures the crystallinity increase is significant for most polymers containing higher comonomer amounts: 23–28% (EB5-V at −6 °C), 12–17% (EH11 at −6 °C), 36–42% (EO5 at −2 °C), 21–25% (EO6 at −7 °C), 26–31% (ETD2 at −5 °C), 16–22% (EB6 at −10 °C), and 37–46% (EOD2 at −6 °C) and still higher crystallinities can be obtained at lower temperatures for many of these studied copolymers. The polymer EB6, which according to our recent investigations [40] does not exhibit any diffraction peaks in its WAXS spectrum and therefore lacks any lamellar structures, show increasing crystallinities at sub-zero temperatures.

From the results of the ethylene–1-hexene copolymers in Fig. 8 and the results in Table 1, we note that although we were not able to observe any peak in the original melting scan of the rather highly branched copolymer EH6, the temperature-dependent curve obtained with a lower starting temperature reveals that crystallinity exists at lower temperatures.
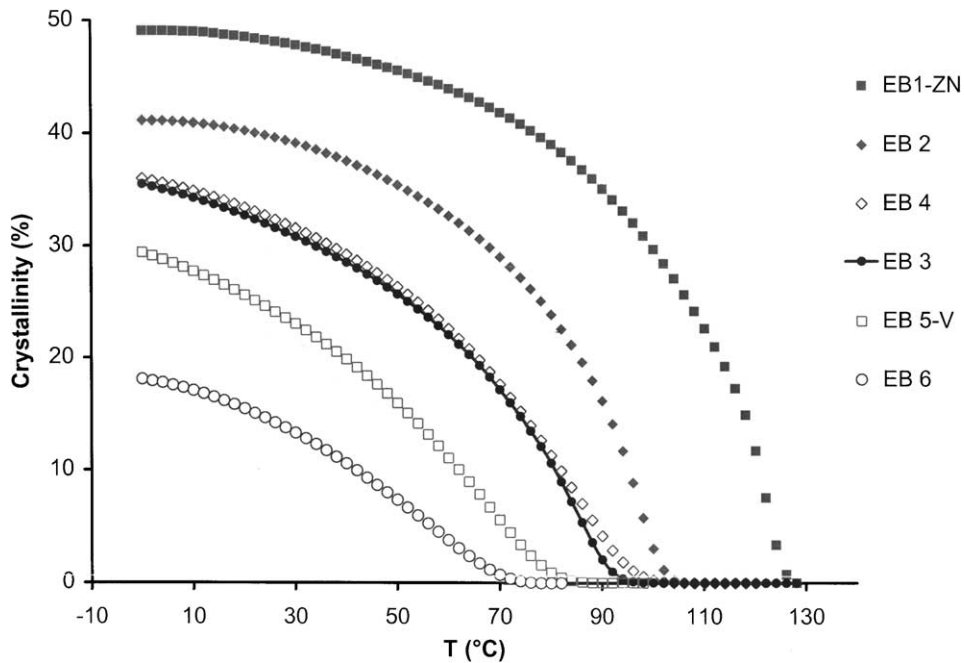
Fig. 7. Temperature-dependent crystallinity curves of ZN- and Me-catalyzed ethylene–1-butene copolymers.

Fig. 9 displays selected crystallinity curves of ethylene–1-octene copolymers and ethylene/long chain copolymers. The EVCH copolymers show a slightly higher T_R temperature at equivalent comonomer content, which is in accordance with our earlier findings [37] and the results in Table 1, demonstrating a less pronounced decrease in melting temperature and crystallinity of ethylene–vinylcyclohexane copolymers compared with those of ethylene–1-hexene or ethylene–1-hexadecene. This difference was suggested to be a result of the bulky, randomly distributed vinylcyclohexane rings, which do not disturb the ordering
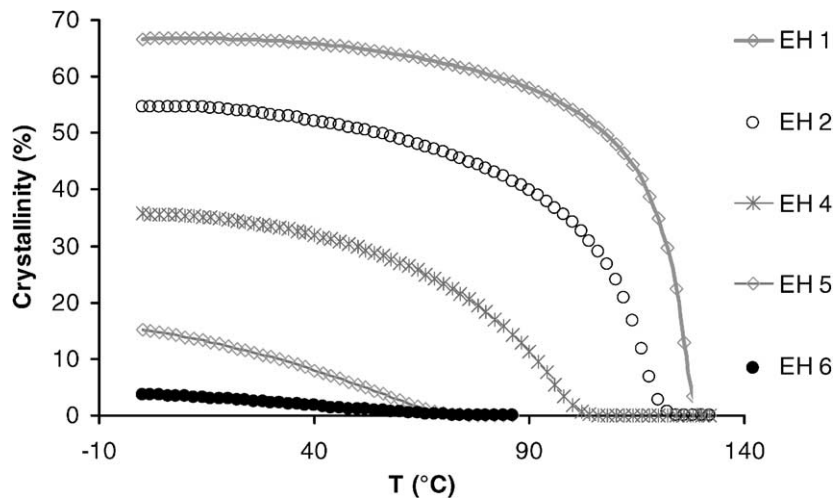

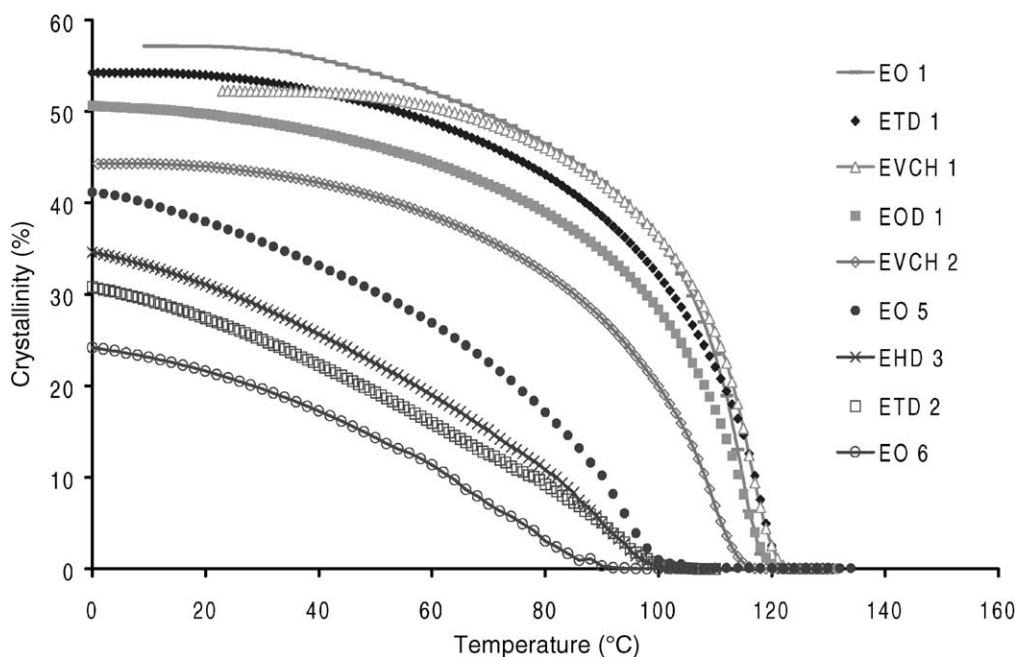Fig. 8. Temperature-dependent crystallinity curves of Me-catalyzed ethylene–1-hexene copolymers.

Fig. 9. Temperature-dependent crystallinity of Me-catalyzed ethylene–1-octene and ethylene/long chain olefin copolymers.

of the polymer in the same extent as the other como-nomers. The copolymers EO5, EHD3, ETD 2 and EO6, containing larger comonomer amounts, all show rather similar temperature-dependent crystallinity curves. This is not unexpected, as Alamo et al. [47,48] have reported that the chemical nature of branch type (greater than methyl) does not influence the crystallinity level when compared at the same branching content and molecular weight. The mole-cular weights of our Me copolymers in this study are with some exceptions very close to each other. How-ever, the degree of crystallinity is controlled by the crystallizable sequence distribution, and may be affected by the type of catalyst for copolymerization [28,45].

5. Conclusions

SSA and SC give useful information about the heterogeneity and homogeneity in the comonomer distributions of ZN- and Me-catalyzed ethylene–α-copolymers. Our findings are in agreement with those of Müller et al. [14]; that SSA gives a better separation of the segregated peaks obtained after the melting stage, compared with SC. This benefit is most sig-nificant in the segregation of more branched molecular species at lower temperatures. Moreover, SSA pro-vides faster analysis times, which also recently is reported by Lustiger et al. [21].

The extrapolation method used for the determina-tion of crystallinities confirms that, at ambient, espe-cially the Me-catalyzed copolymers contain a lot of material, which can crystallize at lower temperatures. ZN copolymers reach more easily an initial crystal-linity region, where a further decrease in temperature only has an insignificant increase in crystallinity. This is due to the significant amount of linear or less branched species, present in ZN copolymers.

The techniques discussed above have now been applied in our further studies on Me isotactic poly-propylene copolymers.

References

[1] A.P. Gray, K. Casey, Polym. Lett. 2 (1964) 381.
[2] L. Wild, Adv. Polym. Sci. 98 (1990) 1.
[3] B. Monrabal, J. Appl. Polym. Sci. 62 (1994) 491.

[4] T. Kamiya, T. Ishikawa, S. Kambe, N. Ikegami, H. Nishibu, T. Hattori, Proceedings of the SPE Technical Papers, Antec 90, 871 pp.

[5] E. Adisson, M. Ribeiro, A. Deffieux, M. Fontanille, Polymer 33 (1992) 4337.

[6] M. Keating, E.T. Cord, Thermochim. Acta 243 (1994) 129.

[7] M. Keating, I.-H. Lee, C.S. Wong, Thermochim. Acta 284 (1996) 47.

[8] P. Starck, Polym. Int. 40 (1996) 11.

[9] R.A. Shanks, K.M. Drummond, Proceedings of the SPE Technical Papers, Antec 98, 2004 pp.

[10] P. Starck, P. Lehmus, J.V. Seppälä, Polym. Eng. Sci. 39 (1999) 1444.

[11] K.M. Drummond, J.L. Hopewell, R.A. Shanks, J. Appl. Polym. Sci. 78 (2000) 1009.

[12] F. Chen, R.A. Shanks, G. Amarasinghe, Polymer 42 (2000) 4579.

[13] R.A. Shanks, J. Amarasinghe, J. Therm. Anal. 59 (2000) 471.

[14] A.J. Müller, Z.H. Hernandez, M.L. Arnal, J.J. Sanchez, Polym. Bull. 39 (1997) 465.

[15] M.L. Arnal, Z.H. Hermandez, M. Matos, J.J. Sanchez, G. Mendez, A. Sanchez, A. Müller, Proceedings of the SPE Technical Papers, Antec 98, 2007 pp.

[16] M.L. Arnal, J.J. Sanchez, A.J. Müller, Proceedings of the SPE Technical Papers, Antec 99, 2329 pp.

[17] M.L. Arnal, V. Balsamo, G. Ronca, A. Sanchez, A.J. Müller, E.C. Canizales, C.U. de Navarro, J. Therm. Anal. 59 (2000) 451.

[18] H. Wigum, L. Tangen, J.A. Støvneng, E. Rytter, J. Polym. Sci. A 38 (2000) 3161.

[19] W. Liu, S. Kim, J. Lopez, B. Hsiao, M.Y. Keating, I.-H. Lee, B. Landes, R.S.J. Stein, J. Therm. Anal. Calorimetry 59 (2000) 245.

[20] C. Gabriel, D. Lilge, Polymer 40 (2001) 297.

[21] A. Lustiger, J.B.P. Soares, C.L.P. Shan, Proceedings of the SPE Technical Papers, Antec 2001, 1835 pp.

[22] P. Starck, C. Lehtinen, B. Löfgren, Die Angew. Macromol. Chem. 249 (1997) 115.

[23] C. Lehtinen, P. Starck, B. Löfgren, J. Polym. Sci. A 35 (1997) 307.

[24] P. Starck, B. Löfgren, Eur. Polym. J. 38 (2002) 97.

[25] P. Starck, B. Löfgren, J. Mater. Sci. 35 (2000) 4439.

[26] R.A.C. Deblieck, V.B.F. Mathot, J. Mater. Sci. Lett. 7 (1988) 1278.

[27] V.B.F. Mathot, M.F.J. Pijpers, Thermochim. Acta 151 (1989) 241.

[28] V.B.F. Mathot, M.F.J. Pijpers, J. Appl. Polym. Sci. 39 (1990) 979.

[29] V.B.F. Mathot (Ed.), in: Calorimetry and Thermal Analysis of Polymers, Carl Hanser, New York, 1994, p. 105 (Chapter 5).

[30] M. Peeters, B. Goderis, C. Vonk, H. Reynaers, V. Mathot, J. Polym. Sci. B 35 (1997) 2689.

[31] V.B.F. Mathot, R.L. Scherrenberg, T.F.J. Pijpers, Polymer 39 (1998) 4541.

[32] V.B.F. Mathot, Thermochim. Acta 355 (2000) 1.

[33] S.Y. Lai, G.W. Knight, Antec Proc. 51 (1993) 1188.

[34] J. Koivumäki, G. Fink, J.V. Seppälä, Macromolecules 27 (1994) 6254.

[35] A. Malmberg, E. Kokko, P. Lehmus, B. Löfgren, J.V. Seppälä, Macromolecules 31 (1998) 8448.

[36] P. Lehmus, E. Kokko, O. Härkki, R. Leino, H.J. Luttikhedde, J.H. Näsman, J. Seppälä, Macromolecules 32 (1999) 3547.

[37] P. Starck, B. Löfgren, J. Macromol. Sci. Part B-Phys. 41 (2002) 579.

[38] B. Wunderlich, G. Czornyj, Macromolecules 10 (1977) 910.

[39] B. Fillon, J.L. Wittman, B. Lotz, A. Thierry, J. Polym. Sci. B 31 (1993) 1383.

[40] Anon., Temperature-dependent crystallinity software (Windows 95/NT), Jointly Developed by DSM Research B.V., and Anatech B.V., Perkin-Elmer Part No. N520-0050.

[41] V.B.F. Mathot, J. Therm. Anal. 64 (2001) 15.

[42] J. Minick, A. Moet, A. Hiltner, E. Baer, S.P. Chum, J. Appl. Polym. Sci. 58 (1995) 1371.

[43] K. Jokela, A. Väänänen, M. Torkkeli, P. Starck, R. Serimaa, B. Löfgren, J. Seppälä, J. Polym. Sci. B 39 (2001) 1860.

[44] M.Y. Keating, I.-H. Lee, J. Macromol. Sci. Phys. B 38 (1999) 379.

[45] A. Alizadeh, L. Richardson, J. Xu, S. McCartney, H. Marand, Macromolecules 32 (1999) 6221.

[46] T.F. McKenna, Eur. Polym. J. 34 (1998) 1225.

[47] R.G. Alamo, E.K.M. Chan, L. Mandelkern, I.G. Voight-Martin, Macromolecules 25 (1992) 6381.

[48] J.R. Isasi, J.A. Haigh, J.T. Graham, L. Mandelkern, R.G. Alamo, Polymer 41 (2000) 8813.